

# Molecular Spin-Flip Loss and a Dual Quadrupole Trap

David Reens,<sup>\*</sup> Hao Wu,<sup>\*</sup> Tim Langen,<sup>†</sup> and Jun Ye

*JILA, National Institute of Standards and Technology and the University of Colorado and  
Department of Physics, University of Colorado, Boulder, Colorado 80309-0440, USA*

(Dated: August 17, 2017)

Doubly dipolar molecules exhibit complex internal spin-dynamics when electric and magnetic fields are both applied. Near magnetic trap minima, these spin-dynamics lead to enhancements in Majorana spin-flip transitions by many orders of magnitude relative to atoms, and are thus an important obstacle for progress in molecule trapping and cooling. The effect is strongest for Hund's case (a) states and is significant for Hund's case (b) as well. We study these internal spin-dynamics with OH molecules and devise a trap geometry where spin-flip loss can be tuned from over  $200 \text{ s}^{-1}$  to below our  $2 \text{ s}^{-1}$  vacuum limited loss rate with only a simple external bias coil and with no sacrifice of trap strength.

The ultracold regime extends toward molecules on many fronts [1]. KRb molecules have reached lattice quantum degeneracy [2] and other bialkalis continue to progress [3–6]. Creative and carefully engineered laser cooling strategies are tackling certain nearly vibrationally diagonal molecules [7–13]. A diverse array of alternative strategies have succeeded to greater or lesser extents on other molecules [14–20]. All of these molecules will require secondary strategies like evaporation or sympathetic cooling to make further gains in phase space density [21–23]. They also may face a familiar challenge: spin flip loss near the zero of a magnetic trap, but dramatically enhanced for many doubly dipolar molecules due to their internal spin dynamics in mixed electric and magnetic fields.

The knowledge of spin flips or Majorana hops as an eventual trap lifetime limit predates the very first magnetic trapping of neutrals [24]. Spin flips were directly observed near  $50 \mu\text{K}$  and overcome with a time-orbiting potential trap [25] and a plugged dipole trap [26], famously enabling the first production of Bose-Einstein condensates. Motivated by the interest in dipolar molecules in mixed fields for quantum chemistry, precision measurement and many-body physics, we previously investigated loss of magnetically trapped hydroxyl radicals (OH) with applied electric field [27]. This trap loss occurred for sub-states of OH's  $X^2\Pi_{J=3/2}$  ground state manifold other than the most well trapped one (positive parity and full spin polarization,  $|f, m_J=3/2\rangle$ , blue in Fig. 1). Due to the closely spaced parity doublet, a general feature of Hund's case (a), these states intersect opposite parity states at non-zero B-fields, where E-field can open avoided crossings and cause trap loss. We now identify internal spin-dynamics leading to trap loss near  $B=0$  even for the most well trapped state and even at 50 mK.

These internal spin-dynamics are subtle, having eluded three previous investigations of note: In [28] the analogues of atomic spin-flip loss for molecules in mixed fields were modeled, and a magnetic quadrupole trap for OH molecules with superposed E-field was specifically addressed. It was concluded that no significant loss en-

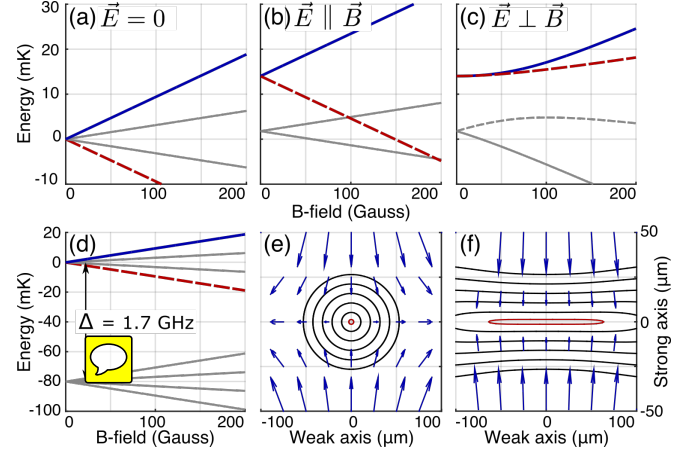




FIG. 1. A uniform E-field, added to magnetically trapped molecules for dipolar studies or other purposes, can lead to spin-flip losses. Four Zeeman split lines in OH's  $X^2\Pi_{3/2}$  manifold are shown (a-c), with the trapped  $|f, 3/2\rangle$  state in blue and its spin-flip partner  $|f, -3/2\rangle$  in dashed red. These states are shown with no E-field (a), with  $E = 150 \text{ V/cm}$  and  $E \parallel B$  (b), and with  $E \perp B$  (c). Note the vastly reduced red-blue splitting in the latter case. The gray close dashes (c) denote the  $|f, 1/2\rangle$  state, which is briefly discussed in the main text. The opposite parity ( $|e\rangle$ ) manifold is split by  $\Delta$  (d). Energy splitting contours are shown every 40 MHz near the zero of a 2 T/cm magnetic quadrupole trap for OH molecules [27] without E-field (e), and with uniform  $E = 150 \text{ V/cm}$  along the strong axis of the quadrupole (f). The vectors are  $\mu_{\text{eff}}\vec{B} \pm d_{\text{eff}}\vec{E}$ , where the sign is positive above the horizontal centerline and negative below, which represents the proper quantization axis for magnetically trapped molecules. Note the drastic widening of the lowest contour (red), the culprit for molecular spin-flip loss enhancement.

hancement due to electric field would be evident. This is true only for the approximate  $^2\Pi_{1/2}$  Hamiltonian used in that study. In [29] E-fields were applied in our magnetic quadrupole trap to study E-field induced collisions. Although an initial approximation was made of the spin-dynamical effect, subsequent investigations have revealed it to be a threefold underestimate, enough to render de-

convolution of any remaining collision  effect difficult. Finally, in [30] it was correctly noted that Hund's case (a) molecules maintain a quantization axis in mixed fields. The states of the molecule were shown to align with one of the two quantization axes given by the vectors  $\mu_{\text{eff}}\vec{B} \pm d_{\text{eff}}\vec{E}$ ,  $\mu_{\text{eff}}$  and  $d_{\text{eff}}$  the effective dipole moments of the molecule in uncombined fields. It was asserted that this would maintain quantization near the zero of a quadrupole trap and avoid spin-flip loss, but as we now describe the loss is actually enhanced.

We begin with an intuitive explanation of the loss enhancement based on molecular orientation. Consider a magnetic quadrupole trap, where a weak-field seeking molecule remains trapped insofar as it adiabatically follows the field direction. When molecules pass near the trap center, they experience a rotating field direction, causing spin-flips. When electric field is added, it dominates in the trap center where the magnetic field is weakest. ~~Quantization is maintained but the quantization axis does not rotate with the magnetic field. As correctly noted in [30], this causes a quantization axis to be maintained, either of  $\mu_{\text{eff}}\vec{B} + d_{\text{eff}}\vec{E}$ . Now suppose a molecule initially follows the sum quantization axis and is in a region where  $E$  and  $B$  are nearly parallel before passing by the trap center. After passing the trap center,  $B$  rotates nearly  $180^\circ$ , so that  $E$  and  $B$  are nearly anti-parallel. Now the length of the sum quantization axis, which is proportional to the field induced energy shift of the molecule, actually decreases with increasing  $|B|$ . Further away from the trap center the molecule is then magnetically strong field seeking and is lost. To avoid loss, the molecule must switch from the vector sum quantization axis to the vector difference quantization axis, so as to remain magnetically weak field seeking despite the change in relative orientation of the fields. To be more precise be more general,~~ we define the relative orientation of the fields as the sign of  $\phi = \vec{E} \cdot \vec{B}$ . When  $\phi$  is negative (positive), the trapped state must have the vector difference (sum) quantization axis, and vice versa, so that an increase in magnitude of the magnetic field increases its energy. ~~Orientation changes whenever internal energy. Whenever  $\phi$  changes sign, i.e. where  $\phi = 0$  which means  $\vec{E} \perp \vec{B}$ . This happens in a 2D region, since, there will be a chance of spin-flip associated with the molecule's propensity to maintain its quantization axis rather than remain on the highest energy doubly weak field seeking branch. Since  $\phi$  is a continuous scalar defined in 3D,  $\phi = 0$  is a contour level of the 3D scalar valued function  $\phi$  one of it's contour levels and thus always corresponds to a 2D surface; in the case of a magnetic quadrupole with homogeneous  $E$  it is a plane.~~ 

We can quantify by diagonalizing the molecular Hamiltonian in mixed fields to find the energy splitting between the well trapped substate. This intuition is in agreement with a more rigorous analysis of the

energy splittings between the trapped state and its spin-flip partner (Fig. 1a-e). The preceding quantization axis discussion suggests that spin-flips occur when crossing the  $\phi = 0$  planar region, so we expect a correspondingly reduced energy splitting there, since this splitting controls the likelihood of spin-flips along a molecule's trajectory via the Landau-Zener formula. This is indeed the case; compare panels (b-e). In fact, by series expanding the exact eigenenergies of OH. By exactly diagonalizing the approximate eight state ground molecular Hamiltonian for OH, subtracting the relevant state energies and Taylor expanding, we find  $H_{E \perp B}(B) \approx (\mu_{\text{eff}}B)^3 \Delta^2 / (d_{\text{eff}}E)^4 + \Delta$ .

$$H(B_{\perp}, B_{\parallel}, E) = (\mu_{\text{eff}}B_{\perp})^3 \Lambda^2 / (d_{\text{eff}}E)^4 + \mu_{\text{eff}}B_{\parallel} \quad (1)$$

Here the magnetic field is considered in parallel and perpendicular components relative to the electric field, and  $\Lambda$  is the lambda doubling,  $B = |\vec{B}|$ , and  $E = |\vec{E}|$ . The relevant splitting between spin flip partner states reaches a deep minimum whenever  $B_{\parallel}$  goes to zero and  $\vec{E} \perp \vec{B}$ , where the remaining Zeeman splitting is no longer linear, but cubic. This means the energy splitting will be small in a much larger region surrounding the zero of a magnetic quadrupole trap than otherwise reduced from linear to cubic in magnetic field (Fig. 1e-f).


We can develop a scaling law for the loss enhancement this causes: a molecule of thermally average velocity  $v$  passing close enough to the trap center to have an energy splitting below  $\kappa = \sqrt{\hbar \dot{H}}$ ,  $\dot{H}$  the rate of approach of the energy levels  $2\mu_{\text{eff}}B'v$  and  $B'$  the trap gradient, will flip with probability at least  $1/e$ . a-c). This reduction in the Zeeman splitting from linear to cubic is in fact a well known phenomenon in the precision measurement community [31, 32], and experimentalists have exploited it for the suppression of unwanted influence from magnetic fields in measurements of the electron electric dipole moment. However, in the case of applying mixed fields during trapping, this suppression is not beneficial but rather detrimental, because the reduced splitting greatly expands the region in which spin-flips can occur (Fig. 1e-f). The extent of the loss enhancement is best addressed as discussed below, but a reasonable scaling law can be formed by comparing the surface area of energy contours such as those shown in red in Fig. 1e-f. For 50 mK OH in our previous 2 T/cm magnetic quadrupole [33],  $\kappa$  is 5 MHz. The region near the trap center where the splitting is below  $\kappa$  is initially an ellipsoid with radii  $\kappa / (\mu_{\text{eff}}B')$ , but broadens in the two directions where by the energy scale of hops without any application of electric field, electric field enhances the factor one obtains by setting  $H_{E \perp B}(B) = \kappa$  and solving for  $B$ . The resulting increase in flux through the ellipsoid comes by squaring,  $\eta = (d_{\text{eff}}E / \sqrt{\kappa \Delta})^{8/3}$ . Thus, E-fields beyond  $\sqrt{\kappa \Delta} / d_{\text{eff}}$  lead to almost cubic 

TABLE I. Enhancements ( $\eta$ ) and loss rates ( $\Gamma$ ) for OH with typical applied fields. Zero field values are equivalent to atomic spin-flip loss. E-field is required during evaporation and spectroscopy to open avoided crossings for  $|e\rangle$  parity states [22, 27], or applied for polarization of the molecules to study collisions [29]. Background loss is  $2 \text{ s}^{-1}$ , experiment length 100 ms.

$E \text{ (V/cm)}$	55 mK		5 mK		Purpose
	$\eta$	$\Gamma \text{ (s}^{-1}\text{)}$	$\eta$	$\Gamma \text{ (s}^{-1}\text{)}$	
0	1	0.02	1	1.3	Zero Field
300	5	0.1	9	11	Evaporation
550	17	0.3	40	50	Spectroscopy
3000	1000	19	1600	2000	Polarizing

enhancements in spin-flip loss for OH (Tab. I). This new understanding modifies our interpretation of evaporation data for OH [22], especially at 5 mK where the loss rate is significantly enhanced by the  $E$ -fields used for RF knife purposes. We do find enhancements in normalized density at low fields for shallow RF knife cuts from 55–30 mK, by  $\eta = (d_{\text{eff}} E / \sqrt{\kappa} \Delta)^{8/3}$ .

Generalizing beyond OH, Hund's case (a) states exhibit reduced Zeeman splittings near  $B=0$  when that are not always cubic as for OH but satisfy  $H_{E \perp B}(B) \propto (\mu_{\text{eff}} B)^{2m_J}$ . Only states with  $m_J=1/2$  retain a linear Zeeman splitting, but they are either not well trapped if  $J=1/2$  also, or they are initially linear until avoided crossings with other states (e.f. Fig. 1e). This bears out in all test Hamiltonians we have diagonalized, and can be understood intuitively as follows: the Zeeman effect is a perturbation on a Hamiltonian whose quantization axis, which defines the  $|m_J\rangle$  quantum number, has already been set by  $\vec{B}$ . We can better quantify the extent of the expansion by considering molecular trajectories in light of the Landau Zener formula:

$$P_{\text{hop}} = e^{-\Delta^2 / \hbar \dot{H}} \quad (2)$$

Which relates the probability of diabatically hopping between two states  $P_{\text{hop}}$  to the Stark effect. Normally the Zeeman effect would linearly split states according to  $|m_J\rangle$ , but from its perspective the states are superpositions  $|m_J\rangle \pm |-m_J\rangle$  and do not split at all to first order. Only via perturbations of energetic coupling between the states  $\Delta$  and the rate of approach of the energy levels  $\dot{H}$ . Any molecules whose trajectory passes through the  $\vec{E} \perp \vec{B}$  surface experience a minimum energy splitting  $\Delta$  at the point of intersection with the plane. The rate of approach of the levels  $\dot{H}$  near this intersection is given simply by the projection of the molecule velocity on the normal to the plane, which dominates over the parallel contribution except for molecules moving almost entirely in that direction, an unlikely situation.

Moreover, although the Landau-Zener formula assumes infinitely linear energy level approach before and after a crossing, the cubically suppressed energy gap at the crossing is much less than the average energy of a trapped molecule, so that to a good approximation its velocity hardly changes in the regime where the energy splitting is small. With these simplifying observations, it becomes possible to approximate the hopping probability for a molecule knowing only its crossing point and orthogonal velocity. By assuming a thermal distribution, the Landau Zener probability can be numerically integrated over the instantaneous spatial distribution in the plane and the Maxwellian velocity distribution orthogonal to the eigenbasis itself does a Zeeman splitting emerge. plane to obtain a spin-flip loss flux out of the trap. We perform such integrations for OH in our previous 2 T/cm magnetic quadrupole [33] under various electric fields of interest (Tab. I).

Beyond Hund's case (a), any state exhibiting competition between  $E$ -fields and  $B$ -fields for alignment of the molecule will be susceptible. One way to avoid competition is for the fields to couple to unrelated parts of the Hamiltonian, which happens to a limited extent for Hund's case (b) states without electron orbital angular momentum ( $\Sigma$  states,  $\Lambda=0$ ) [30]. In these states, which include most laser-cooled and alkali molecules thus far, the  $E$ -fields and  $B$ -fields couple to rotation and spin respectively, which are only related by the spin-rotation coupling constant  $\gamma$ . Where the field-induced shifts are large compared with  $\gamma$ , they stop competing, and both lead to linear energy shifts regardless of the magnitude of the other. This means that the cross sectional area of loss regions is enhanced by  $(\gamma/\kappa)^2$  but is then bounded. Typical molecules have  $\gamma$  in the tens of MHz [23], and  $\kappa$  much lower than the 5 MHz for our warm and very tightly confined OH; so

Unfortunately, experimental verification of this model and these loss-flux calculations is difficult in a magnetic quadrupole trap with superimposed electric field because of an important competing effect: the enhanced field dependent collision cross-section. Furthermore, our prior results on the collisional effect [29] might be largely explained by the enhanced spin-flip loss enhancement remains important. In some cases, e.g. for YO [34], certain hyperfine states avoid spin-flip loss entirely. These states are characterized by significant electron-spin-to-nuclear-spin dipolar coupling, which results in a protective gap regardless of field orientation, which makes experimental verification especially important. Alarmed by this possibility, we developed a new trap where the enhanced molecular spin-flip loss can be conclusively experimentally demonstrated without any convoluted collisional effects, and where our loss-flux calculations could be clearly tested.

We can generalize to arbitrary geometries and consider

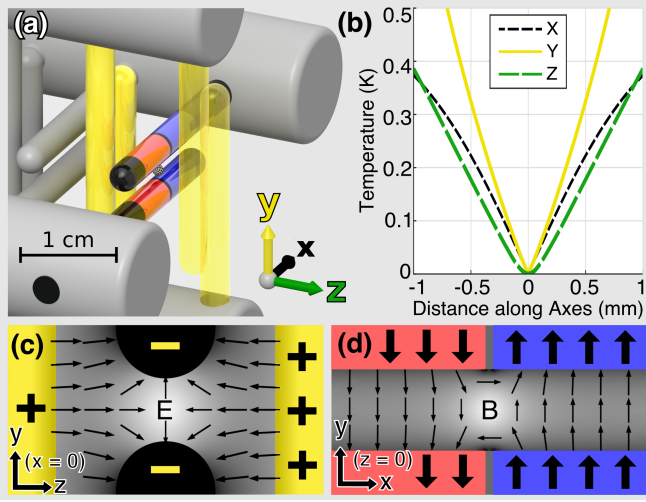


FIG. 2. The last six pins of our Stark decelerator [33] form the trap (a), which is 0.45 K deep with trap frequency  $\nu \approx 4$  kHz (b). Along  $y$  the trap is bounded by the 2 mm pin spacing. The yellow pins are positively charged and the central pin pair negatively, which forms a 2D electric quadrupole trap with zero along the  $x$ -axis. This is shown for the  $x=0$  plane (c), with yellow pins artificially projected for clarity since they don't actually intersect the plane. The central pins are magnetized, with two domains each. Blue indicates magnetization along  $+\hat{y}$ , red along  $-\hat{y}$ . These domains produce a magnetic quadrupole trap with zero along the  $z$ -axis, shown in the  $z=0$  plane (d).

methods to suppress the loss using a simple strategy: avoid  $\mu_{\text{eff}}B < d_{\text{eff}}E$  where . One way to achieve this is to trap with E-field and superpose B-field. The lambda doublet prevents flips in this configuration, but it correspondingly rounds the trap minimum, weakening confinement. Another option is to trap with both fields and keep zeros precisely overlapped. This was realized for OH with a superposed magnetic quadrupole and electric hexapole [35]. Such a scheme prevents loss enhancement, but does not remove it entirely. Another possibility is to use one field only, but any experiment which aims to make use of the doubly dipolar nature of molecules cannot accept this compromise.

We opt for a new geometry: a

Our idea is to use a pair of 2D quadrupole traps, one magnetic and the other electric, with orthogonal centerlines (Fig. 2):

$$\vec{B} = B'x\hat{y} - B'y\hat{x} \quad \vec{E} = E'y\hat{y} - E'z\hat{z} \quad (3)$$

We achieve these fields in a geometry that matches our Stark decelerator [16]. This approach is similar to the Ioffe-Pritchard strategy [36], where a 2D magnetic quadrupole is combined with an axial magnetic dipole trap. While this successfully prevents spin-flip loss, axial and radial trapping interfere, resulting in significantly lower trap depths than for a 3D quadrupole. We

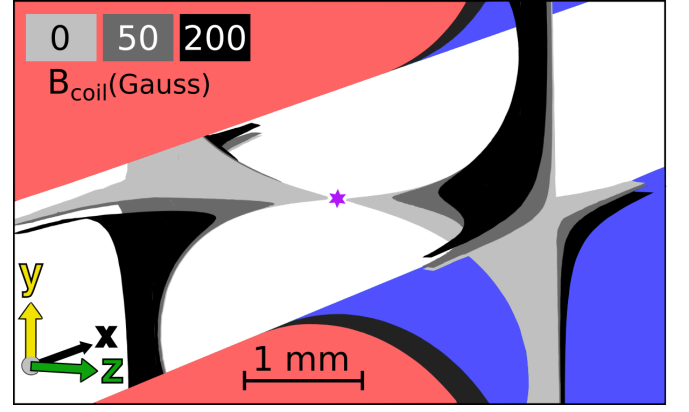


FIG. 3. Surfaces where spin-flips can occur ( $\vec{E} \perp \vec{B}$ ,  $\mu_{\text{eff}}B < d_{\text{eff}}E$ ) are shown for three values of  $B_{\text{coil}}$  in light gray, dark gray, and black. The magnetic pins are shown as in Fig. 2 for context. The purple star marks the trap center, to which molecules are confined within a  $\sim 1$  mm diameter.

thwart this interference by using electric field for the third direction. Our This geometry has  $\vec{E} \perp \vec{B}$  in the two planes  $x=y=0$  both the  $x=0$  and  $y=0$  planes, and  $\mu_{\text{eff}}B < d_{\text{eff}}E$  in a large cylinder surrounding the  $z$ -axis—a perfect recipe for large spin-flip losses. However, by adding a small magnetic field  $\vec{B} = B_{\text{coil}}\hat{z}$  along the centerline of the magnetic quadrupole with an external bias coil, a fully tunable scenario emerges dramatic change can be made to the surfaces where  $\vec{E} \perp \vec{B}$  with only a tiny change to the trapping potential.

Adding  $B_{\text{coil}}$  only slightly rounds the magnetic trapping potential, but it  $B_{\text{coil}}$  morphs the  $\vec{E} \perp \vec{B}$  surface from a pair of planes into a hyperbolic sheet ( $x \cdot y = z \cdot B_{\text{coil}}/B'$ ), pushing it away from the  $z$ -axis where the magnetic field is smallest. Thus, small magnitudes of  $B_{\text{coil}}$  are sufficient to avoid loss.

$$\vec{E} \cdot \vec{B} = B'E'xy - B_{\text{coil}}E'z = 0 \Rightarrow x \cdot y = z \cdot B_{\text{coil}}/B' \quad (4)$$

In Fig. 3, the surfaces where  $\vec{E} \perp \vec{B}$  for several  $B_{\text{coil}}$  magnitudes are shown—calculated wherever the splitting is below the hopping threshold  $\kappa$  there is small enough that a molecule of thermally average velocity orthogonal to the surface would have a  $1/e$  or greater hopping probability. The loss regions are tuned too ought to be tuned far enough from the trap center that molecules cannot access them, yielding a. This is indeed what we observe, note the striking difference in trap lifetime (lifetimes in Fig. 4a). With only 200 G bias field (the trap is 5 kG deep) the loss is suppressed below that due to background gas.

As a further confirmation of our model of the loss, we translate In order to stringently verify our calculations of loss by integration of molecule fluxes



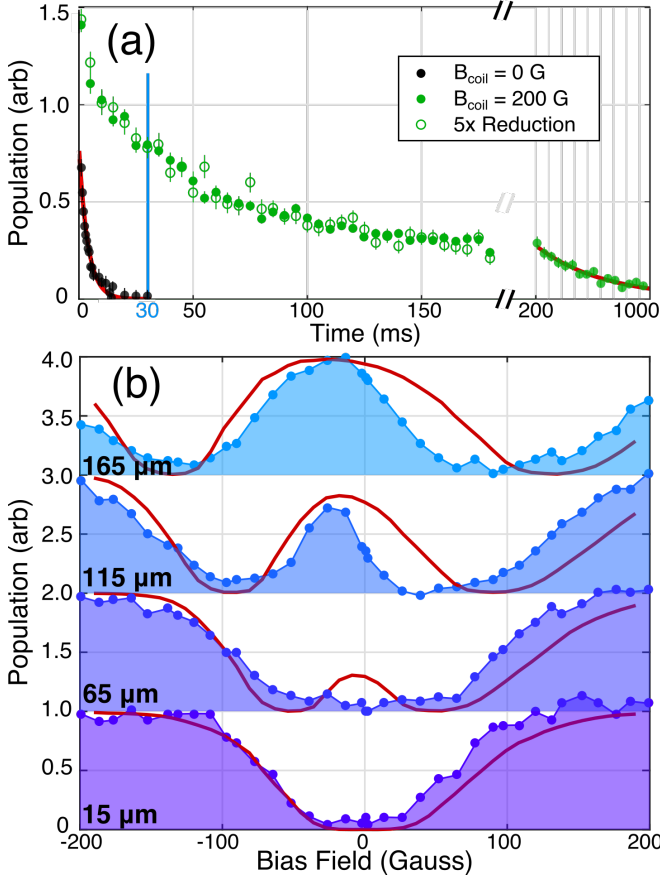


FIG. 4. Time traces (a) without bias field (black), with bias field (green dots), and with modulated density (green circles). One body fits (red) give loss rates of  $200 \text{ s}^{-1}$  without bias field and  $2 \text{ s}^{-1}$  with full bias field at long times, in agreement with our background gas pressure. At the fixed time 30 ms, population is shown as a function of both pin translation and bias field (b), for several values of pin translation, labeled relative to perfect alignment. Fits (red) are calculated by integrating the molecule flux of a thermal ensemble through surfaces where  $\vec{E} \perp \vec{B}$ .

across  $\vec{E} \perp \vec{B}$  surfaces, we perform these calculations for a diverse collection of loss surfaces obtained by translation of the magnetic pins along the  $\hat{x}$  direction in their mounts to alter the surface where, and compare experimental data against expectations (Fig. 4b). This translation serves to disrupt the idealized 2D magnetic quadrupole by adding a small trapping field  $\vec{B} \propto B'z\hat{z}$ . This means that  $B_{\text{coil}}$  no longer directly tunes the magnetic field magnitude along the  $z$ -axis. Instead,  $B_{\text{coil}}$  must first overcome the slight trapping field, translating a point of zero  $B$ -field along the  $z$ -axis and eventually out of the trap. This point has  $\mu_{\text{eff}}B < d_{\text{eff}}E$  and  $\phi = \vec{E} \cdot \vec{B} = 0$ , leading to strong loss unless aligned with the trap center where  $E=0$  also. This means that without  $B_{\text{coil}}$ , the loss should be a local minimum; as  $|B_{\text{coil}}|$  is increased the loss should first worsen and then improve when the zero leaves the trap. This qualitative explanation matches the

observed double well structure in population verses  $B_{\text{coil}}$ .

Quantitatively, we fit the family of curves (red), which dramatically alters the  $\vec{E} \perp \vec{B}$  surfaces and the magnitude of the fields and the hopping probability across them. We perform this same translation in situ, and obtain a striking agreement (Fig. 4b) by assuming a completely time independent and thermal population distribution and integrating molecule flux weighted by Landau-Zener probability over the contorted surfaces where for each  $B_{\text{coil}}$  and pin translation. This idealized calculation nonetheless matches the data with. This is particularly remarkable given that this direct integral calculation assumes a purely thermal distribution and doesn't involve the computation of any actual trajectories. The fits are performed using only temperature as a free parameter, which enters the calculation via the thermal distribution used for integration, and fits to  $170 \pm 20 \text{ mK}$ . [34]. An intuitive explanation for the intriguing double well structure in population verses  $B_{\text{coil}}$  is that  $B_{\text{coil}}$  first translates the magnetic zero along the  $z$ -axis, overlapping it with larger electric fields at first before moving it out of the trap.

Microwave spectroscopy shows that increasing  $B_{\text{coil}}$  increases population and shifts its distribution to higher energy. Triangles indicate the field at which a molecule can access loss regions for a given  $B_{\text{coil}}$ . The dotted lines are eye-guides, but the solid line for highest  $B_{\text{coil}}$  is a fit to  $175 \pm 15 \text{ mK}$ .

We further confirm our model using microwave spectroscopy (Fig. ??), which detects the molecules experiencing a specific  $B$ -field by transferring them to an opposite parity state that is dark to our detection laser, as in [22]. Although the magnetic energy is only part of the total energy of molecules in our dual electric and magnetic quadrupole, molecules with a high magnetic energy during our spectroscopic snapshot are more likely to have a high total energy. It is seen that increasing  $B_{\text{coil}}$  increases population first at low fields.

With strong experimental confirmation of the molecular spin-flip loss enhancement, we can move on to generalize beyond OH. Hund's case (a) states are most susceptible in the sense that smaller electric fields are sufficient to cause a significant problem, but with enough electric field any state exhibiting competition between  $E$ -fields and  $B$ -fields for alignment of the molecule or atom will be susceptible. One way to avoid competition is for the fields to couple to unrelated parts of the Hamiltonian, which happens to a limited extent for Hund's case (b) states without electron orbital angular momentum ( $\Sigma$  states,  $\Lambda=0$ ) [30]. In these states, which include most laser-cooled and alkali molecules thus far, the  $E$ -fields and then at higher fields. This is consistent with our calculations showing that loss location moves further from the trap center with

increasing  $B_{\text{coil}}$  (Fig. 3), and thus can be accessed only by higher energy molecules. At largest  $B_{\text{coil}}$  the distribution fits to  $175 \pm 15$  mK, agreeing with the pin translation fits (Fig. 4b). B-fields couple to rotation and spin respectively, which are only related by the spin-rotation coupling constant  $\gamma$ . Since  $\gamma$  is usually in the tens of MHz [23], molecular spin-flip loss remains quite significant. The inclusion of hyperfine requires a careful case-by-case investigation. For OH, it would initially seem to add an extra splitting that could protect from spin-flips, but in fact the lossy plane is only shifted slightly away from  $\vec{E} \perp \vec{B}$  but retains the same area. For YO [37], certain hyperfine states avoid spin-flip loss entirely. These states are characterized by significant electron-spin-to-nuclear-spin dipolar coupling, which results in a protective gap regardless of field orientation.

In the case of lowest applied B-field in Fig. ??, a negative signal is observed. This indicates an  $|e\rangle$  state accumulation. We can also generalize to arbitrary geometries with a simple loss suppression strategy: avoid  $\mu_{\text{eff}} B < d_{\text{eff}} E$  where  $\vec{E} \perp \vec{B}$ . This is maximally violated by the magnetic quadrupole, where in a suitably small region even the smallest stray electric field dominates the magnetic. One trivial tactic would be to use only one field, but we note that one of the main attractions of working with dipolar species is to utilize both. Another way is to trap with E-field and superpose B-field. Unlike the Zeeman effect, the Stark effect is never linear, and some zero field parity splitting always prevents the orientation reversing spin-flips we have discussed connect  $|f, 3/2\rangle$  to  $|f, -3/2\rangle$ , the latter experiences various avoided crossings due to the large electric confinement fields and remains weakly trapped. Its field-dressed state character varies, transitioning to  $|e, 3/2\rangle$  at larger B-fields (Fig. 1d) that we have been discussing for magnetic traps. However, this same splitting pushes all states with the same sign of  $m_J$  very close to one another, leading to a different type of loss [38]. Intriguingly, this kind of electric trap loss is not necessarily worsened by the addition of magnetic field but can be totally mitigated by it [39]. Another option is to trap with both fields and keep zeros precisely overlapped. This was realized for OH with a superposed magnetic quadrupole and electric hexapole [35].

The present trap, in addition to providing our desired experimental testing ground for molecular spin-flip loss, also manages to provide large 5 T/cm trap-gradients useful for maintaining high densities and collision rates. Moreover, with loss removed, we observe a population trend whose initially fast decay rate decreases over time (Fig. 4a, green dots), suggesting collisions. To test this, we implement a five-fold reduction in initial population [40] and scale the resulting trend by five (green circles). If collisions had contributed, this

new trend would show less decay, but we observe no significant change. This absence of collisions differs from our earlier work [22], which as we have mentioned shows signatures of evaporation for shallow cuts. This but could be attributed to a the significantly higher initial temperature and correspondingly lower density, reduced molecule number, or differences in trap geometry and loading, in this trap. However, the results of this paper introduce a need for new interpretation of other aspects of this evaporation work, since the electric fields used for the RF knife ought to have caused a significant effect to the distribution. We discuss the implications further in supplementary materials. An alternative hypothesis for the population trend is the existence of chaotic trap orbits with long escape times [41]. Moving forward, we aim to increase the density by means of several improvements [42, 43].

Molecule enhanced spin-flip loss arises in mixed electric and magnetic fields due to a competition between field quantization axes where and  $\mu_{\text{eff}} B < d_{\text{eff}} E$ . We conclusively demonstrate this effect and overcome it and suppress this effect using our dual magnetic and electric quadrupole trap. Our explanation of the effect provides, which is also an ideal setting for further progress in collisional physics thanks to its large trap gradient. Our calculation of the magnitude of spin-flip loss via flux through surfaces where  $\vec{E} \perp \vec{B}$  enables detailed predictions of how its location and magnitude ought to scale with bias field and trap alignment, which we experimentally verify. Our results correct existing predictions about molecular spin-flips in mixed fields and pave the way toward further improvements in molecule trapping and cooling.

We acknowledge the Gordon and Betty Moore Foundation, the ARO-MURI, JILA PFC, and NIST for their financial support. T.L. acknowledges support from the Alexander von Humboldt Foundation through a Feodor Lynen Fellowship. We thank J.L. Bohn, S.Y.T. van de Meerakker, and M.T. Hummon for helpful discussions. We thank Goulven Quémener for his continued involvement in this research.

\* Contributed equally. Email dave.reens@colorado.edu or hao.wu@colorado.edu.

† Present Address: 5. Physikalisches Institut und Center for Integrated Quantum Science and Technology (IQST), Universität Stuttgart, Pfaffenwaldring 57, 70569 Stuttgart, Germany

- [1] L. D. Carr, D. DeMille, R. V. Krems, and J. Ye, New Journal of Physics **11**, 055049 (2009).
- [2] S. A. Moses, J. P. Covey, M. T. Miecnikowski, B. Yan, B. Gadway, J. Ye, and D. S. Jin, Science **350**, 659 (2015).
- [3] T. Takekoshi, L. Reichsöllner, A. Schindewolf, J. M. Hutson, C. R. Le Sueur, O. Dulieu, F. Ferlaino, R. Grimm,

- and H.-C. Nägerl, *Physical Review Letters* **113**, 205301 (2014).
- [4] J. W. Park, S. A. Will, and M. W. Zwierlein, *Physical Review Letters* **114**, 205302 (2015).
- [5] M. Guo, B. Zhu, B. Lu, X. Ye, F. Wang, R. Vexiau, N. Bouloufa-Maafa, G. Quémener, O. Dulieu, and D. Wang, *Physical Review Letters* **116**, 205303 (2016).
- [6] L. R. Liu, J. T. Zhang, Y. Yu, N. R. Hutzler, Y. Liu, T. Rosenband, and K.-K. Ni, “Ultracold Molecular Assembly,” (2017), arXiv:1701.03121.
- [7] B. K. Stuhl, B. C. Sawyer, D. Wang, and J. Ye, *Physical Review Letters* **101**, 243002 (2008).
- [8] E. S. Shuman, J. F. Barry, and D. DeMille, *Nature* **467**, 820 (2010).
- [9] M. T. Hummon, M. Yeo, B. K. Stuhl, A. L. Collopy, Y. Xia, and J. Ye, *Physical Review Letters* **110**, 143001 (2013).
- [10] J. F. Barry, D. J. McCarron, E. B. Norrgard, M. H. Steinecker, and D. DeMille, *Nature* **512**, 286 (2014).
- [11] V. Zhelyazkova, A. Cournol, T. E. Wall, A. Matsushima, J. J. Hudson, E. A. Hinds, M. R. Tarbutt, and B. E. Sauer, *Physical Review A* **89**, 053416 (2014).
- [12] M. H. Steinecker, D. J. McCarron, Y. Zhu, and D. DeMille, *ChemPhysChem* **17**, 3664 (2016).
- [13] B. Hemmerling, E. Chae, A. Ravi, L. Anderegg, G. K. Drayna, N. R. Hutzler, A. L. Collopy, J. Ye, W. Ketterle, and J. M. Doyle, *Journal of Physics B: Atomic, Molecular and Optical Physics* **49**, 174001 (2016).
- [14] J. M. Doyle, J. D. Weinstein, R. DeCarvalho, T. Guillet, and B. Friedrich, *Nature* **395**, 148 (1998).
- [15] H. L. Bethlem, G. Berden, and G. Meijer, *Physical Review Letters* **83**, 1558 (1999).
- [16] J. R. Bochinski, E. R. Hudson, H. J. Lewandowski, G. Meijer, and J. Ye, *Physical Review Letters* **91**, 243001 (2003).
- [17] E. Narevicius, A. Libson, C. G. Parthey, I. Chavez, J. Narevicius, U. Even, and M. G. Raizen, *Physical Review Letters* **100**, 093003 (2008).
- [18] A. Wiederkehr, H. Schmutz, M. Motsch, and F. Merkt, *Molecular Physics* **110**, 1807 (2012).
- [19] A. Prehn, M. Ibrügger, R. Glöckner, G. Rempe, and M. Zeppenfeld, *Physical Review Letters* **116**, 063005 (2016).
- [20] Y. Liu, M. Vashishta, P. Djuricanin, S. Zhou, W. Zhong, T. Mittertreiner, D. Carty, and T. Momose, *Physical Review Letters* **118**, 093201 (2017).
- [21] L. P. Parazzoli, N. J. Fitch, P. S. Zuchowski, J. M. Hutson, and H. J. Lewandowski, *Physical Review Letters* **106**, 1 (2011).
- [22] B. K. Stuhl, M. T. Hummon, M. Yeo, G. Quémener, J. L. Bohn, and J. Ye, *Nature* **492**, 396 (2012).
- [23] G. Quémener and J. L. Bohn, *Physical Review A - Atomic, Molecular, and Optical Physics* **93**, 1 (2016).
- [24] A. L. Migdall, J. V. Prodan, W. D. Phillips, T. H. Bergeman, and H. J. Metcalf, *Physical Review Letters* **54**, 2596 (1985).
- [25] W. Petrich, M. H. Anderson, J. R. Ensher, and E. A. Cornell, *Physical Review Letters* **74**, 3352 (1995).
- [26] K. B. Davis, M. O. Mewes, M. R. Andrews, N. J. van Druten, D. S. Durfee, D. M. Kurn, and W. Ketterle, *Physical Review Letters* **75**, 3969 (1995).
- [27] B. K. Stuhl, M. Yeo, B. C. Sawyer, M. T. Hummon, and J. Ye, *Physical Review A* **85**, 033427 (2012).
- [28] M. Lara, B. L. Lev, and J. L. Bohn, *Physical Review A* **78**, 033433 (2008).
- [29] B. K. Stuhl, M. Yeo, M. T. Hummon, and J. Ye, *Molecular Physics* **111**, 1798 (2013).
- [30] J. L. Bohn and G. Quémener, *Molecular Physics* **111**, 1931 (2013).
- [31] M. A. Player and P. G. H. Sandars, *Journal of Physics B: Atomic and Molecular Physics* **3**, 1620 (1970).
- [32] J. J. Hudson, B. E. Sauer, M. R. Tarbutt, and E. A. Hinds, *Physical Review Letters* **89**, 023003 (2002).
- [33] B. C. Sawyer, B. K. Stuhl, D. Wang, M. Yeo, and J. Ye, *Physical Review Letters* **101**, 203203 (2008).
- [34] ~~This is particularly relevant given the recently realized 3D MOT for YO.~~
- [35] B. C. Sawyer, B. L. Lev, E. R. Hudson, B. K. Stuhl, M. Lara, J. L. Bohn, and J. Ye, *Physical Review Letters* **98**, 1 (2007).
- [36] D. E. Pritchard, *Physical Review Letters* **51**, 1336 (1983).
- [37] This is particularly relevant given the recently realized 3D MOT for YO.
- [38] T. E. Wall, S. K. Tokunaga, E. a. Hinds, and M. R. Tarbutt, *Physical Review A - Atomic, Molecular, and Optical Physics* **81**, 1 (2010).
- [39] S. A. Meek, G. Santambrogio, B. G. Sartakov, H. Conrad, and G. Meijer, *Physical Review A - Atomic, Molecular, and Optical Physics* **83** (2011), 10.1103/PhysRevA.83.033413.
- [40] Microwaves couple opposite parities during deceleration, giving a uniform loss probability across the molecular distribution.
- [41] R. González-Férez, M. Iñarrea, J. P. Salas, and P. Schmelcher, *Physical Review E* **90**, 062919 (2014).
- [42] U. Even, *EPJ Techniques and Instrumentation* **2**, 17 (2015).
- [43] Y. Segev, N. Bibelnik, N. Akerman, Y. Shagam, A. Luski, M. Karpov, J. Narevicius, and E. Narevicius, *Science Advances* **3**, e1602258 (2017).